Carbohydrate Polymers 123 (2015) 99–104

Contents lists available at ScienceDirect

Carbohydrate Polymers

journal homepage: www.elsevier.com/locate/carbpol

Mechanical and thermal properties of *Posidonia oceanica* cellulose nanocrystal reinforced polymer

Fedia Bettaieb[a,b,c], Ramzi Khiari[a,b,c], Alain Dufresne[b,c,*], Mohamed Farouk Mhenni[a], Mohamed Naceur Belgacem[b,c]

[a] Research Unity of Applied Chemistry & Environment, Department of Chemistry, Faculty of Sciences, University of Monastir, 5019, Tunisia
[b] Univ Grenoble Alpes, LGP2, F-38000 Grenoble, France
[c] CNRS, LGP2, F-38000 Grenoble, France

ARTICLE INFO

Article history:
Received 30 November 2014
Received in revised form 9 January 2015
Accepted 12 January 2015
Available online 20 January 2015

Keywords:
Cellulose nanocrystal
Posidonia oceanica
Nanocomposite
Dynamic mechanical analysis
Aspect ratio

ABSTRACT

In the present study, cellulose nanocrystals (CNC) were isolated from *Posidonia oceanica* balls and leaves. CNC was prepared from this marine biomass by sulfuric acid hydrolysis (H_2SO_4) treatment. The raw fibers were firstly isolated by a delignification-bleaching process then the acid hydrolysis treatment was performed at 55 °C during 40 min under mechanical stirring. The ensuing CNCs were characterized by their morphological and thermal properties using transmission electron microscopy (TEM) and thermal gravimetric analysis (TGA), respectively. Nanocomposite materials using the CNC extracted from marine biomass were obtained by casting and evaporating a mixture of this suspension with poly(styrene-co-butyl acrylate). The effect of CNC loading on mechanical and thermal properties was studied. Dynamic mechanical analysis (DMA) results showed a strong reinforcing effect of CNC that depends on their origin (balls or leaves). The difference was attributed not only to differences in the aspect ratio of CNC but also to the stiffness of the percolating network of nanoparticles.

1. Introduction

Nanotechnology has rapidly become a multidisciplinary field and one of the faster growing research areas is the preparation of cellulose-based nanoparticles (CNPs). Cellulose nanowhiskers (CNWs), or nanocrystals (CNCs), can be extracted from any bioresource, especially from wood, as well as from annual plants and residues of agricultural crops such as corn grain, sugarcane bagasse, corn cobs, wheat stems, and seed coats using top-down technologies. In recent years, nanocellulose-based composites attracted much interest because of their significantly enhanced mechanical properties versus neat polymers or conventional polymer composites (Dufresne, 2012; Hussain, Hojjati, Okamoto, & Gorga, 2006; Ibrahim, El-Zawawy, & Nassar, 2010). Abundance, high strength and stiffness, low weight and biodegradability are some special useful features of nanoscale cellulose fiber materials which make them promising candidates for bio-nanocomposite production (Siró & Plackett, 2010). Isolation, characterization, and search for applications of novel forms of cellulose, variously termed crystallites, nanocrystals, nanowhiskers, nanofibrils, and nanofibers, is generating much activity currently. Isolated cellulosic materials with at least one dimension in the nanometer range are referred to generically as nanocellulose.

Nanocellulose is able to combine important cellulose properties such as hydrophilicity, broad chemical-modification capacity, and the formation of versatile semicrystalline fiber morphologies with the specific features of nanoscale materials, mainly caused by the very large surface area of these materials. As a reinforcing agent for composite materials, this biopolymer displays attractive advantages such as renewability, recyclability and biodegradability. In addition, it has intrinsic good mechanical properties and its price is relatively lower compared to synthetic fibers.

As described for the first time by Rånby and Ribi (1950), colloidal aqueous CNC suspensions can be obtained by controlled sulfuric acid-catalyzed degradation of cellulose fibers (Anglès & Dufresne, 2000; De Rodriguez, Thielemans, & Dufresne, 2006; Pei, Zhou, & Berglund, 2010; Tang & Weder, 2010; Wang, Tian, & Zhang, 2010). Since this earlier work the production of CNCs has been investigated extensively in the literature from a variety of natural cellulosic sources (Dufresne, 2012), and it was found that the dimensions of ensuing nanoparticles usually depend on the origin of the starting cellulose materials and hydrolysis conditions. For example, CNC from wood is 3–15 nm in width and 100–200 nm in

* Corresponding author at: Univ. Grenoble Alpes, LGP2, F-38000 Grenoble, France. Tel.: +33 476826995.
E-mail address: alain.dufresne@pagora.grenoble-inp.fr (A. Dufresne).

http://dx.doi.org/10.1016/j.carbpol.2015.01.026
0144-8617/

length (Beck-Candanedo, Roman, & Gray, 2005; Pu, Zhang, Elder, Deng, Gatenholm et al., 2007), while those obtained from *Valonia*, a sea plant, are reported to be 20 nm in width and 1000–2000 nm in length (Hanley, Giasson, Revol & Gray, 1992; Revol, 1982). Similarly, the average dimensions of crystallites produced from cotton are between 4 and 10 nm in diameter and 100–300 nm in length (Shafizadeh & McGinnis, 1971). In addition, tunicate, a sea animal, gives particles of ca. 10–20 nm in width and 500–2000 nm in length (Anglès & Dufresne, 2000).

Cellulose is one of the most abundant natural polymers on Earth. Each year, between 10^{10} and 10^{11} tons of this biopolymer is produced (Azizi Samir, Alloin, Sanchez, & Dufresne, 2004; Lavoine, Desloges, Dufresne, & Bras, 2012). Cellulosic fibers are widely used for many purposes such as in textile industries, pharmaceutical applications, packaging, paper making and innovative applications (green composites). As a result, the consumption of this natural fiber increases exponentially (Khiari, Marrakchi, Belgacem, Mauret, & Mhenni, 2011a; Khiari, Mauret, Belgacem, & Mhenni, 2011b). In order to satisfy the important demand, various renewable sources are needed. In this context, the exploitation of cellulosic biopolymer obtained from annual plants and/or agricultural waste (vine stems, date palm rachis etc. . .) is a new strategy that is adopted in numerous countries (Abrantes, Amaral, Costa, & Duarte, 2007; Antunes, Amaral, & Belgacem, 2000; Bendahou et al., 2008; Cordeiro, Belgacem, Torres, & Mourad, 2004; Fiserova, Gigac, Majtnerova, & Szeiffova, 2006; Shatalov, Quilho, & Pereira, 2001). Tunisia is characterized by its limited arable area and reduced forest resources. Nevertheless, other cellulosic biomass can be valorized such as marine wastes. In fact, Tunisia has about 1300 km of Mediterranean coast and a large quantity of *Posidonia oceanica* is accumulated every year. Every summer the beaches must be cleaned to satisfy the touristic clientele. This plant represents one of the most important productions of the coastal zone in the Mediterranean basin and especially in Tunisia (Ott, 1980). This aquatic plant *P. oceanica*, is widely distributed, fast-growing, and available in large quantity on Mediterranean coasts and its valorization as cellulosic fibers has been studied (Aguir & Mhenni, 2006; Khiari, Mhenni, Belgacem, & Mauret, 2010; Khiari, Marrakchi et al., 2011a; Khiari, Mauret et al., 2011b). We recently reported the preparation of CNC from cellulose extracted from the leaves and balls from *P. oceanica* (Bettaieb et al., 2015). The processing and characterization of nanocomposite materials obtained from these cellulosic nanoparticles and an amorphous polymeric matrix are investigated in the present study.

2. Materials & methods

2.1. Materials

The *P. oceanica* balls and leaves (POB and POL, respectively) were obtained from Skanes-Monastir (Tunisia). Sodium hydroxide (99% purity) was used for alkaline treatment. Sodium chlorite, acetic acid, and sodium hydroxide were used as bleaching agents whereas the sulfuric acid was used for hydrolysis treatment. All chemicals were purchased from Sigma-Aldrich and were used without further purification. The polymer acrylic latex dispersion was a commercial product from MPC-PROKIM (Tunisia). It consists of styrene (S - 35 wt%) and butyl acrylate (BA - 5 wt%). The size of the polymer particles was around 140 nm, the glass transition was around 30 °C and the solid content was 50 wt%.

2.2. Preparation of CNC from P. oceanica

Different steps are needed to accomplish the preparation of CNC from POL and POB. Fig. 1 schematically illustrates these various steps leading to the preparation of the two kinds of CNC. The detailed procedure is reported in our earlier study (Bettaieb et al., 2015).

Briefly, 10 g of prepared cellulose purified from POL or POB was dispersed in 200 mL of 6.5 mol L^{-1} sulfuric acid in a flask containing a mechanical stirrer and a thermometer. Hydrolysis treatment was performed at 55 °C under vigorous stirring for 40 min. The removal of excess acid was achieved by repeated centrifugation steps with distilled water and dialysis against distilled water for 72 h using a cellulose acetate membrane (Sigma-Aldrich) until neutral pH, i.e. 6–7. The suspension was then submitted to an ultrasonic treatment for 5 min to reduce the aggregate size and stored in a refrigerator. The hydrolysis yield was calculated as the ratio between the weight of the freeze-dried hydrolyzed residue and the initial weight of starting material. The different CNC preparations were carried out at least in duplicate.

2.3. Preparation of CNC reinforced nanocomposites

Different poly(S-co-BuA) nanocomposite samples reinforced with various amounts of CNC, namely 0, 1, 2, 5, 7, 10 and 15 wt%, were prepared by casting/evaporation using CNC suspensions from *P. oceanica* leaves and balls. First, the CNC suspension was stirred using ultrasonic treatment during 120 s, then the latex was added and the mixture was magnetically stirred for 8 h. Thereafter, the mixture was cast in a Teflon mold and stored at 35 °C. After water evaporation which duration depended on the cellulose content (typically few days) solid nanocomposites films were obtained and conditioned for 24 h under controlled temperature (23 °C) and relative humidity (50%). The entire nanocomposites were prepared at least in triplicate.

2.4. Characterization of CNC from P. oceanica and nanocomposites

The detailed morphological characterization of CNC obtained from POB and POL was reported in our earlier study (Bettaieb et al., 2015). We reported here a more detailed morphological investigation and thermal characterization of CNC, as well as mechanical properties of CNC reinforced nanocomposites films.

2.4.1. Transmission electron microscopy (TEM)

The size (diameter and length) of the elementary particles and their distribution were characterized by transmission electron microscopy (TEM) using JEOL 200CX transmission electron microscope at 80 kV. About 0.5 μL of each suspension corresponding to CNC-POL and CNC-POL was deposited onto a 300 mesh carbon-coated copper grid using a labnet micropipette. Water was allowed to evaporate. Additional drop of each CNC suspension was added onto their respective grid to increase the amount of cellulose particles and the process was repeated.

2.4.2. Thermogravimetric analysis (TGA)

Thermogravimetric analysis (TGA, Perkin-Elmer Pyris 1 TGA-7) of cellulose extracted from *P. oceanica* leaves and balls and ensuing CNC was performed. About 15 mg of obtained sample was put into a platinum sample pan and heated from 25 to 900 °C at a heating rate of 10 °C min^{-1} under a nitrogen atmosphere with a flow rate of 20 mL min^{-1}. The test was repeated at least in duplicate.

2.4.3. Dynamic mechanical analysis (DMA)

The dynamic mechanical analysis (DMA) in tensile mode was used in order to characterize the thermo-mechanical properties of films prepared from CNC obtained from *P. oceanica* (balls and leaves) and poly(S-co-BuA) latex as matrix. The tests were carried out using a RSA 3 DMA apparatus from Rheometrics. The resulting

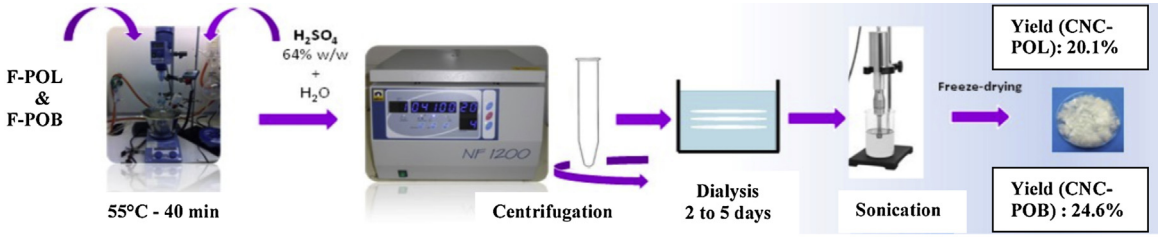

Fig. 1. Schematic representation of the different steps used to prepare CNC from POL and POB.

nanocomposites were cut into thin rectangular strips with dimensions of $30 \times 5 \times 0.4\,mm^3$. The measurements were carried out under isochronal conditions at 1 Hz, and the temperature scanning interval varied from −90 to 100 °C at a heating rate of 2 °C min^{-1}. Measurements were repeated in triplicate.

3. Results and discussions

3.1. CNC from P. oceanica

In our earlier work (Bettaieb et al., 2015), CNC was extracted from *P. oceanica* using an acid hydrolysis treatment (sulfuric acid). The yield values of CNC from *P. oceanica* leaves (CNC-POL) and balls (CNC-POB) were 24.6% and 20.1%, respectively, with respect to the initial weight of the raw material. It is worth to note that the obtained average CNC yield is higher than the one reported for other cellulosic fibers (Dufresne, 2012). The morphological features of CNC extracted from *P. oceanica* leaves and balls were reported in our previous work (Bettaieb et al., 2015).

Fig. 2 shows the TEM observation of CNC and their diameter and length distribution. The dimensions of the corresponding CNC were evaluated by digital image analysis (Image J) of TEM micrographs using a minimum of 100 CNC. The average width of CNC-POL was around 7 nm while the average length was 520 nm. For CNC-POB, the width and the length were around 8 nm and 283 nm, respectively. Therefore, the average aspect ratio (length/width) of CNC-POL and CNC-POB was about 75 and 35, respectively. It is worth noting that the former value is very high and even higher than for CNC extracted from tunicin (67) (Anglès & Dufresne, 2000) and capim dourado (67) (Siqueira, Abdillahi, Bras & Dufresne, 2010) that were considered as the upper limit (Dufresne, 2012).

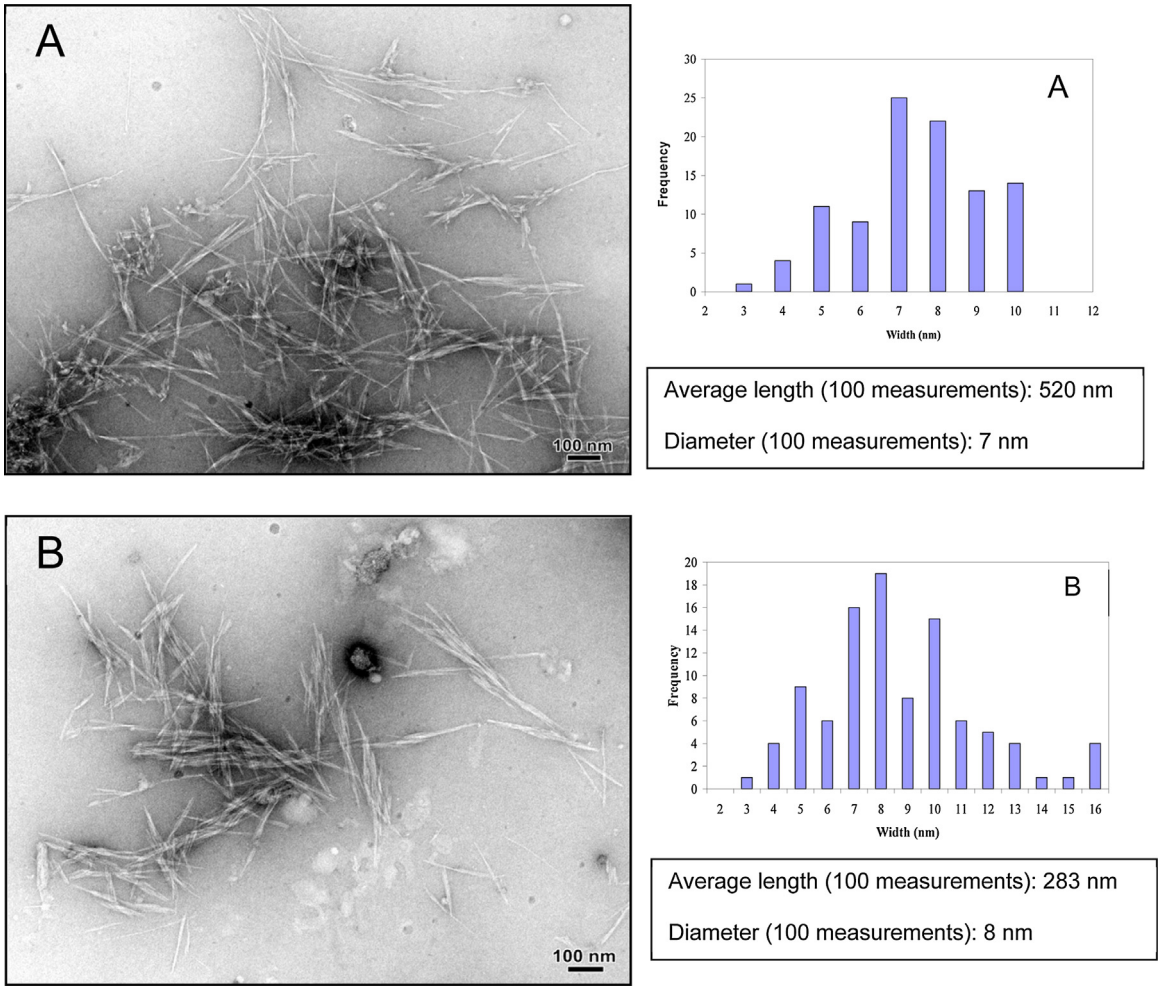

Fig. 2. TEM observation, and length and diameter distribution for CNC-POL (A) and CNC-POB (B).

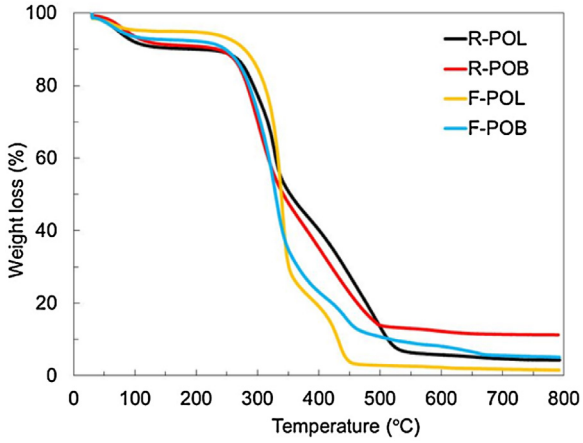

Fig. 3. TGA of the different materials from *Posidonia oceanica*: raw leaves (R-POL) and balls (R-POB), and cellulose fibers purified from the leaves (F-POL) and balls (F-POB).

The thermal degradation of the raw materials and bleached fibers from *P. oceanica* has been investigated by TGA. Fig. 3 show the TGA curves obtained for the raw leaves (R-POL) and balls (R-POB), and purified cellulose fibers from the leaves (F-POL) and balls (F-POB). Around 100 °C a weak weight loss is observed. It is obviously ascribed to moisture evaporation as for any hydrophilic material. Around 250 °C, hemicelluloses (the most thermally unstable compounds) start to degrade. Around 350 °C, the slope of the curve completely differs for the raw materials and purified cellulose fibers indicating a change in the chemical kinetics. The slowing down of the thermal degradation process for raw materials is ascribed to lignin.

The thermal degradation of CNC prepared from *P. oceanica* leaves and balls were also investigated by TGA. Results are reported in Fig. 4. Regardless the source of cellulose from *P. oceanica*, it is clearly seen that compared to the raw starting materials, the isolated nanocrystals CNC-POB and CNC-POL display a significantly reduced thermal stability. As reported in the literature (Lin & Dufresne, 2014; Roman & Winter, 2004), this effect is ascribed to the acid hydrolysis step which generally involves sulfuric acid for suspension stability issues. During the hydrolysis step, sulfate groups are introduced on the surface of the nanocrystals promoting at the same time lowering in thermal stability. It is interesting to note that CNC-POB starts to degrade at lower temperatures compared to CNC-POL. This observation could be related to the difference in specific surface area of the nanorods. Considering the

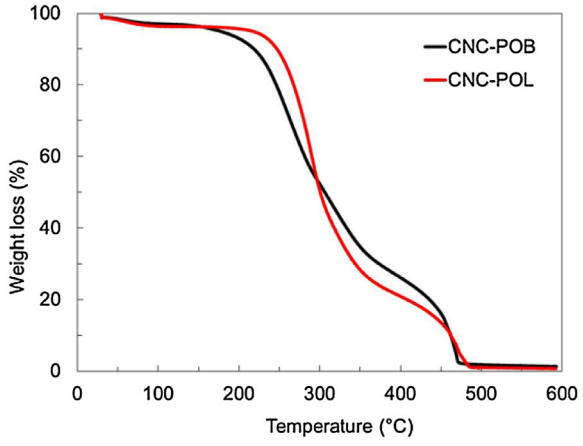

Fig. 4. TGA curves for CNC-POB and CNC-POL.

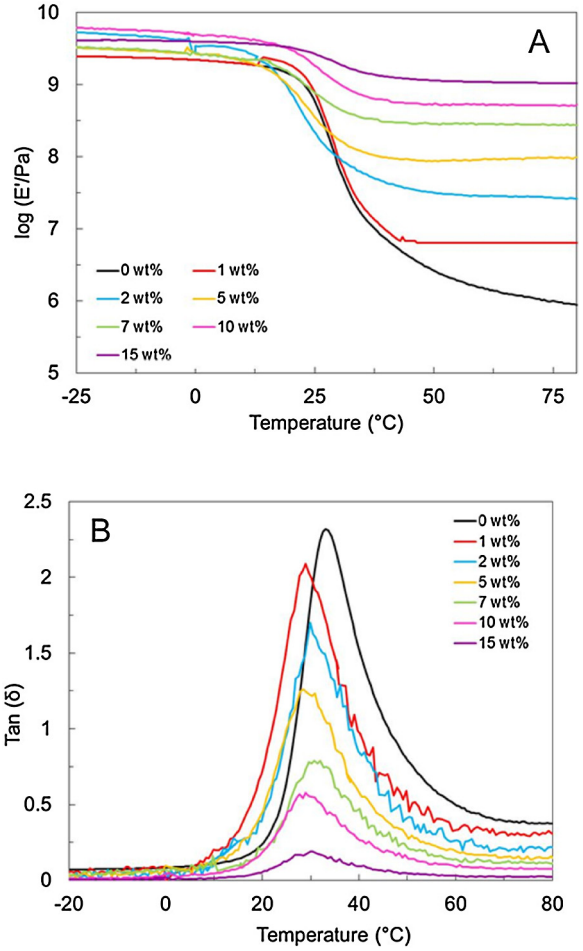

Fig. 5. Evolution of (A) the logarithm of the storage tensile modulus, E′, and (B) loss angle tan δ versus temperature at 1 Hz for nanocomposites based on CNC from POB.

average dimensions for length and diameter and assuming a density of 1.5 g cm^{-3} for crystalline cellulose, the specific surface area for CNC-POB and CNC-POL is around 330 m^2 g^{-1} and 380 m^2 g^{-1}, respectively. Since acid hydrolysis was performed in the same conditions for both cellulosic substrates, one can expect that the density of sulfate groups should be higher for CNC-POB leading to an early thermal degradation. This explanation is consistent with the higher char residue observed for CNC-POB. Indeed, it was shown that increasing the number of sulfate groups on nanocrystals increases the amount of charred residue at 350 °C indicating that sulfate groups are flame-retardant in nature (Roman & Winter, 2004).

3.2. Characterization of CNC reinforced nanocomposite films

The reinforcing potential of CNC from *P. oceanica* leaves and balls was examined by DMA. The evolution of the storage modulus E′ as well as the loss factor (tan δ) as a function of temperature for different CNC contents is shown in Fig. 5a and b, respectively, for CNC-POL.

As expected, the unfilled pol(S-co-BuA) matrix displays a typical behavior of amorphous polymer. At low temperature the polymer is in the glassy state and its storage modulus remains roughly constant around 1 GPa when increasing the temperature. A sharp decrease is observed around 25 °C corresponding to the glass–rubber transition. This relaxation process is also evidenced through a maximum in the mechanical loss factor around 35 °C (Fig. 5b). A weak decrease of the temperature position of the

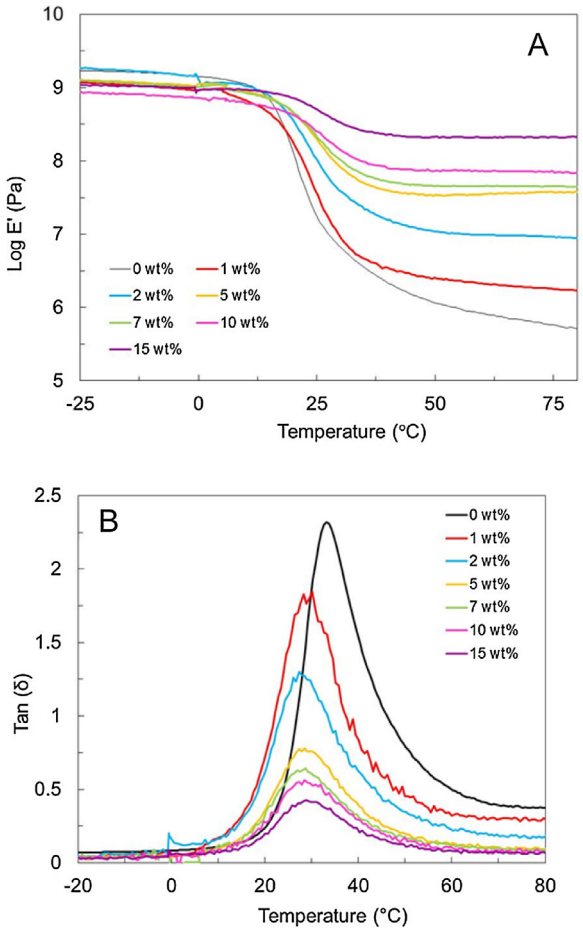

Fig. 6. Evolution of (A) the logarithm of the storage tensile modulus, E′, and (B) loss angle tan δ versus temperature at 1 Hz for nanocomposites based on CNC from POL.

relaxation peak is observed when increasing the CNC content. It is attributed to the well-known mechanical coupling effect. However, the magnitude of the tan δ peak decreases upon CNC addition (Fig. 5b). Above T_g, a significant reinforcing effect of CNC was observed. The curves corresponding to poly(S-co-BuA) nanocomposite films reinforced with CNC-POB are reported in Fig. 6. A higher reinforcing effect is observed for CNC-POL compared to CNC-POB.

This high reinforcing effect could be assigned as already reported in the literature to a mechanical percolation phenomenon of CNC. Above the percolation threshold, the nanoparticles connect and form a stiff continuous network linked through hydrogen bonding (Dufresne, 2012). Slow wet processes such as casting/evaporation were reported to give the highest mechanical performance materials compared to other processing techniques. Indeed, during liquid evaporation strong interactions between nanoparticles can settle and promote the formation of a strong percolating network. It corresponds to the highest mechanical properties that can be reached with CNC for a given polymeric system. This effect was reported to be well predicted from the adaptation of the percolation concept to the classical series-parallel model. Comparison between experimental data and predicted values calculated from the percolation approach can be used to ensure that good dispersion and effective percolation occur. In this model and at sufficiently high temperature, i.e., when the modulus of the matrix is much lower than the one of the percolating network, the elastic modulus of the composite is simply the product of the volume fraction and modulus of the rigid percolating network (Dufresne, 2012).

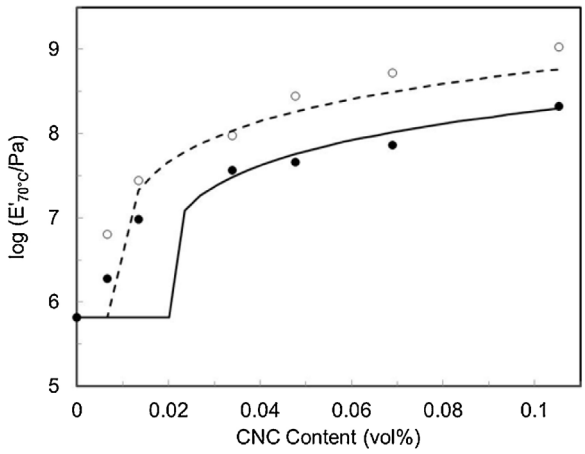

Fig. 7. Evolution of the logarithm of the tensile storage modulus at 70 °C versus CNC content: experimental data for CNC-POB (●) and CNC-POL (○), and predicted data from the percolation approach for CNC-POB (solid line) and CNC-POL (dashed line).

The percolation approach has been used to predict the mechanical performance of CNC-POL and CNC-POB reinforced SBR composites. The volume fraction of the percolating phase can be calculated from the CNC volume fraction, percolation threshold and critical percolation exponent (0.4 for a 3D network). The percolation threshold was determined from the aspect ratio of CNC and the CNC volume fraction was calculated assuming a density of 1 and 1.5 g cm^{-3} for poly(S-co-BuA) and cellulose, respectively. Therefore, CNC-POL with a higher aspect ratio than CNC-POB presents a lower percolation threshold that could explain its higher reinforcing effect. The calculated percolation threshold for CNC-POB and CNC-POL was 2.0 vol% and 0.93 vol%, respectively. Yet, it is well know that for higher CNC contents when a dense cellulosic network can form, the reinforcing effect stabilizes and similar modulus values should be reached regardless the aspect ratio of the nanorods.

However, it was also shown that the stiffness of the CNC percolating network increases when increasing the aspect ratio of the nanoparticles (Bras et al., 2011). Similar observation was reported when comparing the mechanical properties of poly(vinyl acetate) reinforced with CNC extracted from cotton (aspect ratio around 10) and tunicin (aspect ratio around 67) (Shanmuganathan, Capadona, Rowan, & Weder, 2010). From this earlier report (Bras et al., 2011) that showed the evolution of the stiffness of the network as a function of the constitutive CNC and from the aspect ratio of CNC-POB (35) and CNC-POL (75), it can be assumed that the modulus of the percolating network should be around 5 GPa and 16 GPa for CNC-POB and CNC-POL, respectively.

Fig. 7 shows the evolution of the modulus for the composites as a function of the CNC volume content. Both predicted data and experimental rubbery moduli estimated at 70 °C are reported. Below the percolation threshold, the modulus cannot be estimated from the model and the value corresponding to the neat matrix was adopted. It can be clearly observed from this figure that the higher reinforcing observed for CNC-POL compared to CNC-POB can be attributed to both the lower percolation threshold that tends to shift horizontally the modulus values towards lower CNC contents and to the stiffer CNC percolating network that tends to shift vertically the data towards higher modulus values. From a mechanical point of view, it is therefore important to consider high aspect ratio cellulose nanorods, not only because it decreases the percolation threshold and reinforcing capability at low CNC contents, but also because the upper modulus limit corresponding to high CNC contents is higher.

4. Conclusion

In this work, cellulose nanocrystals (CNC) were prepared from *P. oceanica* leaves (POL) and balls (POB) and characterized. CNC with different average width (length) around 7 nm (520 nm) for NCC-POL and 8 nm (283 nm) for NCC-POB were obtained. It corresponds to an average aspect ratio (length/width) for CNC-POL and CNC-POB around 75 and 35, respectively. This allows having CNC extracted from the same source but with very different aspect ratios. Nanocomposite materials were prepared from these CNCs and poly(styrene-co-butyl acrylate) by casting/evaporation. The thermomechanical properties of ensuing composites were characterized and a much higher reinforcing effect was observed in the rubbery state of the polymeric matrix for CNC-POL compared to CNC-POL. From the comparison between experimental and predicted data using the percolation approach it was concluded that the higher aspect ratio of CNC-POL results in both a lower percolation threshold and a stiffer percolating CNC network.

Acknowledgments

The authors gratefully express their sincere gratitude to Dr. Jean Luc PUTAUX, CERMAV Grenoble, France, for his help and availability as well as to “PHC-UTIQUE CMCU” (project 13G1114) and “SSHN 2014-L’Institut français de Tunisie” for their financial support.

References

Abrantes, S., Amaral, M. E., Costa, A. P., & Duarte, A. P. (2007). *Cynara cardunculus* L. alkaline pulps: Alternative fibres for paper and paperboard production. *Bioresource Technology*, *98*, 2873–2878.

Aguir, C., & Mhenni, M. F. (2006). Experimental study on carboxymethylation of cellulose extracted from *Posidonia oceanica*. *Journal of Applied Polymer Science*, *98*, 1808–1816.

Anglès, M. N., & Dufresne, A. (2000). Plasticized starch/tunicin whiskers nanocomposites.1. Structural analysis. *Macromolecules*, *33*, 8344–8353.

Antunes, A., Amaral, E., & Belgacem, M. N. (2000). *Cynara cardunculus* L.: Chemical composition and soda-anthraquinone cooking. *Industrial Crops and Products*, *12*, 85–91.

Azizi Samir, M. A. S., Alloin, F., Sanchez, J. Y., & Dufresne, A. (2004). Cross-linked nanocomposites polymer electrolytes reinforced with cellulose whiskers. *Macromolecules*, *37*, 4839–4844.

Beck-Candanedo, S., Roman, M., & Gray, D. G. (2005). Effect of reaction conditions on the properties and behaviour of wood cellulose nanocrystals suspensions. *Biomacromolecules*, *6*, 1048–1054.

Bendahou, A., Kaddami, H., Sautereau, H., Raihane, M., Erchiqui, F., & Dufresne, A. (2008). Short palm tree fibres polyolefin composites: Effect of filler content and coupling agent on physical properties. *Macromolecular Materials and Engineering*, *293*, 140–148.

Bettaieb, F., Khiari, R., Hassan, M. L., Belgacem, M. N., Bras, J., Dufresne, A., et al. (2015). Preparation and characterization of new cellulose nanocrystals from marine biomass *Posidonia oceanica*. *Industrial Crops and Products*, http://dx.doi.org/10.1016/j.indcrop.2014.12.038

Bras, J., Viet, D., Bruzzese, C., & Dufresne, A. (2011). Correlation between stiffness of sheets prepared from cellulose whiskers and nanoparticles dimensions. *Carbohydrate Polymers*, *84*, 211–215.

Cordeiro, N., Belgacem, M. N., Torres, I. C., & Mourad, J. C. V. P. (2004). Chemical composition and pulping of banana pseudo-stems. *Industrial Crops and Products*, *19*, 147–154.

De Rodriguez, N. L. G., Thielemans, W., & Dufresne, A. (2006). Sisal cellulose whiskers reinforced polyvinyl acetate nanocomposites. *Cellulose*, *13*, 261–270.

Dufresne, A. (2012). Nanocellulose: From Nature to High- Performance Tailored Materials, Berlin/Boston: de Gruyter.

Fiserova, M., Gigac, J., Majtnerova, A., & Szeiffova, G. (2006). Evaluation of annual plants (*Amaranthus caudatus* L., *Atriplex hortensis* L., *Helianthus tuberosus* L.) for pulp production. *Cellulose Chemistry and Technology*, *40*, 405–412.

Hanley, S. J., Giasson, J., Revol, J. F., & Gray, D. G. (1992). Atomic force microscopy of cellulose microfibrils: Comparison with transmission electron microscopy. *Polymer*, *33*, 4639–4642.

Hussain, F., Hojjati, M., Okamoto, M., & Gorga, R. E. (2006). Review article: Polymer–matrix nanocomposites, processing, manufacturing, and application: An overview. *Journal of Composite Materials*, *40*, 1511–1575.

Ibrahim, M. M., El-Zawawy, W. K., & Nassar, M. A. (2010). Synthesis and characterization of polyvinyl alcohol/nanospherical cellulose particle films. *Carbohydrate Polymers*, *79*, 694–699.

Khiari, R., Mhenni, M. F., Belgacem, M. N., & Mauret, E. (2010). Chemical composition and pulping of date palm rachis and *Posidonia oceanica*—A comparison with other wood and non-wood fibre sources. *Bioresource Technology*, *101*, 775–780.

Khiari, R., Marrakchi, Z., Belgacem, M. N., Mauret, E., & Mhenni, M. F. (2011). New lignocellulosic fibres-reinforced composite materials: A step forward in the valorisation of the *Posidonia oceanica* balls. *Composites Science and Technology*, *71*, 1867–1872.

Khiari, R., Mauret, E., Belgacem, M. N., & Mhenni, M. F. (2011). Tunisian date palm rachis used as an alternative source of fibres for papermaking applications. *Bioresources*, *6*, 265–281.

Lavoine, N., Desloges, I., Dufresne, A., & Bras, J. (2012). Microfibrillated cellulose—Its barrier properties and applications in cellulosic materials: A review. *Carbohydrate Polymers*, *90*, 735–764.

Lin, N., & Dufresne, A. (2014). Surface chemistry, morphological analysis and properties of cellulose nanocrystals with gradient sulfation degrees. *Nanoscale*, *6*, 5384–5393.

Ott, J. A. (1980). Growth and production in *Posidonia Oceanica (L.)* Delile. *Marine Ecology*, *1*, 47–64.

Pei, A. H., Zhou, Q., & Berglund, L. A. (2010). Functionalized cellulose nanocrystals as biobased nucleation agents in poly(L-lactide) (PLLA)—Crystallization and mechanical property effects. *Composites Science and Technology*, *70*, 815–821.

Pu, Y., Zhang, J., Elder, T., Deng, Y., Gatenholm, P., & Ragauskas, A. J. (2007). Investigation into nanocellulosics versus acacia reinforced acrylic films. *Composites: Part B*, *38*, 360–366.

Rånby, B. G., & Ribi, E. (1950). Über den feinbau der zellulose. *Experimentia*, *6*, 12–14.

Revol, J. F. (1982). On the cross-sectional shape of cellulose crystallites in *Valonia ventricosa*. *Carbohydrate Polymers*, *2*, 123–134.

Roman, M., & Winter, W. T. (2004). Effect of sulphate groups from sulphuric acid hydrolysis on the thermal degradation behaviour of bacterial cellulose. *Biomacromolecules*, *5*, 1671–1677.

Shafizadeh, F., & McGinnis, G. D. (1971). Morphology and biogenesis of cellulose and plant cell-walls. In R. S. Tipson (Ed.), *Advances in carbohydrate chemistry and biochemistry*. New York: Academic Press.

Shanmuganathan, K., Capadona, J. R., Rowan, S. J., & Weder, C. (2010). Bio-inspired mechanically-adaptive nanocomposites derived from cotton cellulose whiskers. *Journal of Materials Chemistry*, *20*, 180–186.

Shatalov, A. A., Quilho, T., & Pereira, H. (2001). *Arundo donax* L. reed: New perspectives for pulping and bleaching. 1. Raw material characterization. *Tappi Journal*, *84*, 1–14.

Siqueira, G., Abdillahi, H., Bras, J., & Dufresne, A. (2010). High reinforcing capability cellulose nanocrystals extracted from *Syngonanthus nitens* (Capim Dourado). *Cellulose*, *17*, 289–298.

Siró, I., & Plackett, D. (2010). Microfibrillated cellulose and new nanocomposite materials: A review. *Cellulose*, *17*, 459–494.

Tang, L. M., & Weder, C. (2010). Cellulose whisker/epoxy resin nanocomposites. *ACS Applied Materials & Interfaces*, *2*, 1073–1080.

Wang, Y. X., Tian, H. F., & Zhang, L. N. (2010). Role of starch nanocrystals and cellulose whiskers in synergistic reinforcement of waterborne polyurethane. *Carbohydrate Polymers*, *80*, 665–671.